Since January 2020 Elsevier has created a COVID-19 resource centre with free information in English and Mandarin on the novel coronavirus COVID-19. The COVID-19 resource centre is hosted on Elsevier Connect, the company's public news and information website.

European Journal of Radiology 131 (2020) 109256

Contents lists available at ScienceDirect

European Journal of Radiology

journal homepage: www.elsevier.com/locate/ejrad

Can CT performed in the early disease phase predict outcome of patients with COVID 19 pneumonia? Analysis of a cohort of 64 patients from Germany

Stefanie Meiler [a,*], Jan Schaible [a], Florian Poschenrieder [a], Gregor Scharf [a], Florian Zeman [b], Janine Rennert [a], Benedikt Pregler [a], Henning Kleine [c], Christian Stroszczynski [a], Niels Zorger [d], Okka W. Hamer [a,e]

[a] Department of Radiology, Regensburg University Medical Center, Franz-Josef-Strauss-Allee 11, 93053, Regensburg, Germany
[b] Center for Clinical Studies, Regensburg University Medical Center, Franz-Josef-Strauss-Allee 11, 93053, Regensburg, Germany
[c] Department of Pneumology, Hospital Barmherzige Brüder, Prüfeninger Strasse 86, 93049, Regensburg, Germany
[d] Department of Radiology, Hospital Barmherzige Brüder, Prüfeninger Strasse 86, 93049, Regensburg, Germany
[e] Department of Radiology, Hospital Donaustauf, Ludwigstrasse 68, 93093, Donaustauf, Germany

ARTICLE INFO

Keywords:
COVID-19
SARS-CoV-2
Outcome
Prognostic factors
Pneumonia
Computed tomography

ABSTRACT

Purpose: The aim of this study was to investigate if CT performed in the early disease phase can predict the course of COVID-19 pneumonia in a German cohort.
Method: All patients with RT-PCR proven COVID-19 pneumonia and chest CT performed within 10 days of symptom onset between March 1st and April 15th 2020 were retrospectively identified from two tertiary care hospitals. 12 CT features, their distribution in the lung and the global extent of opacifications were evaluated. For analysis of prognosis two compound outcomes were defined: positive outcome was defined as either discharge or regular ward care; negative outcome was defined as need for mechanical ventilation, treatment on intensive care unit, extracorporeal membrane oxygenation or death. Follow-up was performed until June 19th. For statistical analysis uni- und multivariable logistic regression models were calculated.
Results: 64 patients were included in the study. By univariable analysis the following parameters predicted a negative outcome: consolidation ($p = 0.034$), crazy paving ($p = 0.004$), geographic shape of opacification ($p = 0.022$), dilatation of bronchi ($p = 0.002$), air bronchogram ($p = 0.013$), vessel enlargement ($p = 0.014$), pleural effusion ($p = 0.05$), bilateral disease ($p = 0.004$), involvement of the upper lobes ($p = 0.004$, $p = 0.015$) or the right middle lobe ($p < 0.001$) and severe extent of opacifications ($p = 0.002$). Multivariable analysis revealed crazy paving and severe extent of parenchymal involvement to be independently predictive for a poor outcome.
Conclusions: Easy to assess CT features in the early phase of disease independently predicted an adverse outcome of patients with COVID-19 pneumonia.

1. Introduction

In December 2019 a novel coronavirus meanwhile named SARS-CoV-2 was isolated in several patients with acute severe lower respiratory tract illness in Wuhan, Hubei Province, China [1]. The corresponding symptoms were summarized under the term coronavirus disease 2019 (COVID-19). The standard of reference for the diagnosis of COVID-19 is RT-PCR. Initially restricted to Wuhan, the infection spread rapidly reaching the status of a pandemic in March 2020 [2]. Meanwhile over 10 million cases have been confirmed worldwide, among them 194910 in Germany, as of June 29, 2020 [3]. The majority of patients suffering from COVID-19 have no or only mild symptoms and restitute quickly. However, 15 % develop severe pneumonia, and 5% critical disease including acute respiratory distress syndrome (ARDS), septic shock and multi organ failure, eventually leading to death [4].

Several studies reporting the morphology of COVID-19 pneumonia in

* Corresponding author.
E-mail address: stefanie.meiler@ukr.de (S. Meiler).

https://doi.org/10.1016/j.ejrad.2020.109256
Received 15 May 2020; Received in revised form 3 August 2020; Accepted 24 August 2020
Available online 28 August 2020

chest computed tomography (CT) have been published [5–11]. CT features of COVID-19 pneumonia seem to be amazingly similar for many patients. CT morphology can be so suggestive that radiologists might be able to distinguish COVID-19 from pneumonias caused by other viruses [12–15]. However, there are non-infectious differential diagnoses like in particular organizing pneumonia which can look very similar to COVID-19 pneumonia. Regarding sensitivity of CT studies consistently report very high numbers (circa. 95 %) with some of them reporting even higher sensitivities of initial CT as compared to initial RT-PCR [17–19]. Apart from this CT plays an important role for quantification of parenchymal involvement, detection of complications (like pulmonary embolism or superinfection), detection of COVID-19 pneumonia as an "incidental" finding and even for triage in case of constrained resources. Hence, CT has emerged to a widely used tool in the care of patients with suspected or proven COVID-19.

Only few studies evaluated CT features which may allow prediction of course of disease [20–24]. Most of these studies described Chinese cohorts. However, it has to be considered that the course of disease and patient outcome are influenced by many parameters. Among them host features (which again are not only influenced by individual factors but also by ethnicity) and viral genome variability due to mutations might affect outcome. Also organization and resources of the respective health care system determines patient outcome. Thus, evaluation of the prognostic value of CT in a European cohort seems worthwhile. So far there is only one study from Italy linking the amount of parenchymal involvement with patient outcome [25]. Italian hospitals, however, have been intermittently overwhelmed by patient number with consecutive constraints for patient care. Germany so far has been in the fortunate situation to be able to provide sufficient resources at any time.

The aim of this study was to investigate if CT performed in the early disease phase can predict the course of COVID-19 pneumonia and patient outcome in a German cohort.

2. Material and methods

2.1. Study population

This retrospective study was approved by the institutional ethics committee. All procedures performed in studies involving human participants were in accordance with the ethical standards of the institutional and/or national research committee and with the 1964 Helsinki declaration and its later amendments or comparable ethical standards. Written informed consent was waived.

The inclusion criteria were consecutive adult patients (≥18 years old) with RT-PCR positive for SARS-CoV-2 and a chest CT performed within 10 days of symptom onset between March 1st and April 15th 2020. Exclusion criteria were a negative result of RT-PCR for SARS-CoV-2 and non-diagnostic CT, for example due to motion-artifacts. Patients were identified by means of a full-text database query of all CT-scans performed between March 1st and April 15th 2020 using the term "*COVID*" and *SARS* in the Radiological Information System (RIS, Nexus.medRIS, Version 8.42, Nexus, Villingen-Schwenningen, Germany). Patient characteristics (age, gender, comorbidities), symptoms, date of symptom onset, RT-PCR results and patient outcome were extracted from electronic patient records. All patients had at least one CT scan of the chest. In case of several scans per patient the first CT performed per patient was included into the analysis. Patients were followed until June 19th 2020.

2.2. CT protocol

The patients underwent CT scans at two tertiary care hospitals. Chest CTs were performed on two different scanners (16 slice Somatom Sensation 16, 128-slice Definition FLASH, all Siemens Healthcare, Erlangen, Germany). All CT acquisitions were obtained in supine position during end-inspiration. Intravenous contrast material was administered at the discretion of the radiologist considering the individual study indication. Automatic tube voltage selection was applied with a reference tube voltage of 120 kV. Tube current was regulated by an automatic tube current modulation technique with the reference mAs being 40−110. Collimation width was 0.625 mm–0.75 mm. Multiplanar reformations (MPR) were reconstructed in the axial plane with a slice thickness of 0.75–1.5 mm (56 CTs) and 2–4 mm (9 CTs) in lung kernel and with a slice thickness of 1−5 mm in soft tissue kernel. Additional sagittal and coronal MPRs were reconstructed with a slice thickness of 1–3 mm using lung and soft tissue kernel. The pictures were sent to a picture archiving and communication system (PACS, Syngo Imaging, Siemens, Erlangen, Germany).

2.3. Image analysis

Images were analyzed in consensus by two radiologists. The radiologists were blinded to clinical data, laboratory data and patient status. The Fleischner Society definition of CT features were applied when appropriate [26]. The following parameters were analyzed: ground-glass-opacities (GGO, hazy increased opacity of lung with preservation of bronchial and vascular margins), consolidation (homogeneous increase in pulmonary parenchymal attenuation that obscures the margins of vessels and airway walls), crazy-paving pattern (thickened interlobular septa and intralobular lines superimposed on a background of ground-glass opacity), cavities (gas-filled space within consolidation), bronchial dilatation (dilated -with respect to the accompanying pulmonary artery non-tapering bronchus; the term "dilatation" instead of "-ectasis" was intentionally used in order to express that the pathology might be reversible), vessel dilatation (diameter of vessel within or near opacifications clearly larger compared to vessels of the same generation in healthy lung tissue), shape of opacification (round vs curvilinear/band-like vs geographic = opacification outlines the shape of multiple adjacent pulmonary lobules, sharply marginated), margin of opacification (unsharp vs at least to some extent sharp), lung lobes affected. Moreover, distribution of opacifications in the axial plane (predominantly peripheral vs predominantly central and predominantly anterior vs predominantly posterior vs diffuse), lymphadenopathy (diameter >10 mm in short axis) and subjective estimation of extent of parenchymal opacifications (0–33 %: mild, 34–66 %: moderate, 67–100 %: severe) were analyzed.

2.4. Definition of endpoint

Two compound outcomes were defined as the endpoint: positive outcome was defined as either discharge or regular ward care (= group 1); negative outcome was defined to be need for intubation or need for admission to intensive care unit or need for extracorporeal membrane oxygenation (ECMO) or death (group 2).

2.5. Statistical analysis

Age is presented as mean (standard deviation) and all categorical variables as absolute and relative frequencies. Univariable logistic regression models were used to analyze the predictive value of all parameters (demographic data, clinical data, comorbidities and CT findings) on the endpoint (positive vs negative outcome). Furthermore, a multivariable logistic regression model analyzing only the CT findings was calculated. At first, all significant CT findings were added to a model followed by a manual stepwise backward elimination until only predictor variables with $p < 0.1$ were left. A second multivariable model was built the same way including characteristics of parenchymal involvement. Due to quasi-separated data regarding the bronchial dilatation, the penalized likelihood method by Firth [27] was used to reduce the bias of the maximum likelihood estimates. A multivariable model including all CT findings, all grades of parenchymal involvement and further patient related parameters was not feasible due to the

Table 1
Patient characteristics (n = 64).

patient characteristics	patients (n = 64)
age (years)	57.2 (SD 14.5)
time between symptom onlapse and first CT scan (days)	7 (IQR 5–7.25)
gender	
male	40 (62 %)
female	24 (38 %)
symptoms	
fever[a] (>37.5 °C)	47 (75 %)
cough[a]	48 (79 %)
dyspnea[a]	41 (68 %)
fatigue[a]	34 (72 %)
taste dysfunction[a]	11 (25 %)
gastrointestinal[a]	12 (27 %)
comorbidities	
diabetes[a]	8 (12 %)
cardiac failure[a]	3 (5%)
coronary heart disease[a]	6 (9%)
COPD[a]	2 (3%)
asthma[a]	3 (5%)
high blood pressure[a]	23 (37 %)
outcome	
positive (group 1)	31 (48 %)
negative (group 2)	33 (52 %)
death	9 (14 %)

COPD = chronic obstructive pulmonary disease.
[a] Occasional missing values were counted as patients without symptoms/comorbidities.

limited amount of patients and events. Odds ratios and corresponding 95 %-confidence intervals (95 %-CI) were calculated as effect estimates for all logistic regression models. A p-value <0.05 was considered statistically significant. All analyses were performed using R, version 3.6.1 (The R Foundation for Statistical Computing) and SAS, version 9.4 (The SAS institute, Cary, NC.).

3. Results

3.1. Patient demographics and clinical features

64 patients fulfilled the inclusion criteria. The study population included 62 % male (n = 40) and 38 % female (n = 24) patients. Age ranged from 21 to 88 years with a mean of 57.2 years (SD 14.5). Clinical symptoms were fever in 47 patients (75 %), cough in 48 patients (79 %), dyspnea in 41 patients (68 %) and fatigue in 34 patients (72 %). Less frequently seen were gastrointestinal complaints (n = 12; 27 %) and taste dysfunction (n = 11; 25 %). Most common comorbidities were high blood pressure (n = 23, 37 %), diabetes (n = 8, 12 %) and coronary heart disease (n = 6, 9%). Prevalence of obesity and smoking history could not be determined because of frequent lack of corresponding data in patient charts. 9 patients (14 %) deceased during the observation period. Patient characteristics are presented in Table 1.

3.2. CT findings

51 CTs (80 %) were acquired without contrast agent, 13 CTs (20 %) were contrast enhanced. Ground glass opacities (97 %, n = 62) and consolidation (77 %, n = 49) were the most commonly observed patterns. Crazy paving was identified in 25 % of the scans (n = 16). Bronchial dilatation was seen in 14 % (n = 9), air bronchogram in 67 % (n = 43) and vessel enlargement in 48 % (n = 31) of CTs. Pleural effusion was observed in 20 % (n = 13) and lymphadenopathy in 28 % (n = 18) of CTs.

Most of the lesions were at least to some extent sharply marginated (84 %, n = 54). In 30 % of CTs (n = 19) opacifications were curvilinear

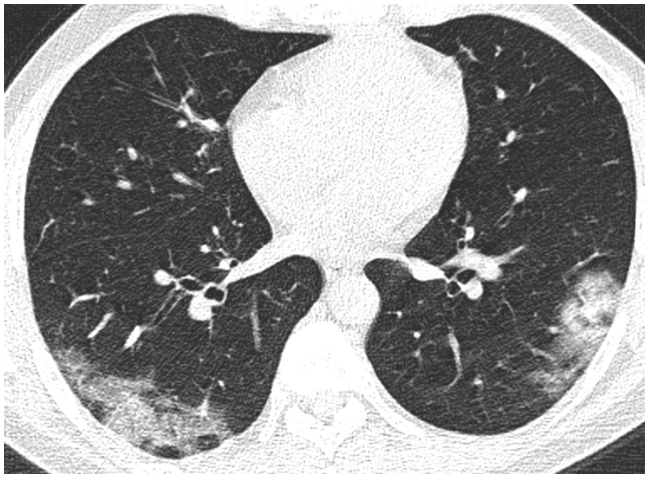

Fig. 1. Mild extent of opacifications. Axial reconstruction of a CT in lung window showing mild affection with ground glass opacities and minor consolidation in the periphery of both lower lobes.

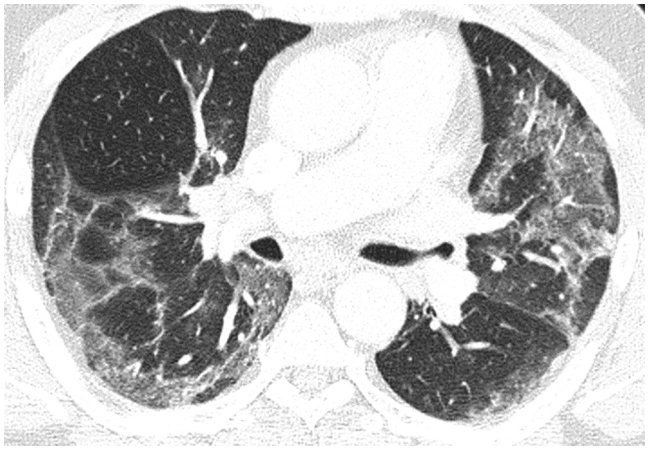

Fig. 2. Moderate extent of opacifications. Axial reconstruction of a CT in lung window showing moderate affection with ground glass opacities in the upper and lower lobes of both lungs.

Fig. 3. Severe extent of opacifications. Axial reconstruction of a CT in lung window showing severe affection with posterior consolidation and adjacent ground glass opacities. Also note the air bronchogram.

Table 2
Frequency of CT features.

CT findings	patients (n = 64)
CT signs	
consolidation	49 (77 %)
GGO	62 (97 %)
crazy paving	16 (25 %)
round shape of opacification	39 (61 %)
sharp margin of opacification	54 (84 %)
geographic shape of opacification	26 (41 %)
curvilinear/bandlike opacification	19 (30 %)
bronchial dilatation	9 (14 %)
air bronchogram	43 (67 %)
cavitation	0
peripheral vessel enlargement	31 (48 %)
pleural effusion	13 (20 %)
lymphadenopathy	18 (28 %)
distribution	
bilateral	57 (89 %)
unilateral	5 (8%)
right upper lobe	57 (89 %)
right middle lobe	54 (84 %)
right lower lobe	61 (95 %)
left upper lobe	52 (81 %)
left lower lobe	59 (92 %)
predominantly peripheral	47 (73 %)
predominantly central	0
diffuse	25 (39 %)
predominantly anterior	2 (3%)
predominantly posterior	53 (83 %)
extent of lung involvement	
mild	26 (41 %)
moderate	23 (36 %)
severe	15 (23 %)
contrast agent	
enhanced scans	13 (20 %)
unenhanced scans	51 (80 %)

shaped, round in 61 % (n = 39) and geographic in 41 % (n = 26). In the vast majority of CTs, lesions were found bilaterally (89 %, n = 57). The right lower lobe (95 %, n = 61) and the left lower lobe (92 %, n = 59) were most often affected. Distribution in the axial plane was predominantly peripheral (n = 47, 73 %) and posterior (83 %, n = 53). In 41 % (n = 26) of CTs extent of opacifications was mild (Fig. 1), in 36 % (n = 23) moderate (Fig. 2) and in 23 % (n = 15) severe (Fig. 3).

CT findings are presented in Table 2.

3.3. Univariable analysis for identification of prognostic relevant CT features

As outlined in the Material and Methods section patients were divided into two groups depending on outcome: Group 1 (care on regular ward or discharge) included 31 patients (48 %). Group 2 (mechanical ventilation/ICU/ECMO/death) included 33 patients (52 %).

3.3.1. Demographic data, clinical data and comorbidities

Dyspnea (OR 3.39, 95 %-CI:1.1, 11.38, p = 0.038) was the only clinical parameter that statistically significantly influenced patient outcome. No comorbidity influenced course of disease. Results are presented in Table 3.

3.3.2. CT findings

Restriction of opacifications to one side (unilateral) (OR n.c., p = 0.022) was the only parameter correlated with a favorable outcome (Fig. 4). Several CT features predicted an adverse outcome: consolidation (OR 3.99, 95 %-CI:1.18,16.06, p = 0.034), crazy paving (OR 10.68, 95 %-CI:2.6,73.12, p = 0.004) (Fig. 5), geographic shape of opacification (OR 3.45, 95 %-CI:1.23, 10.35, p = 0.022), bronchial dilatation (OR

Table 3
Univariable logistic regression to analyze the predictive value of demographic data, clinical data and comorbidities on the primary endpoint (positive vs. negative outcome).

parameter	group 1 (n = 31)	group 2 (n = 33)	odds ratio	p-value
age	55.4 (SD 14.3)	58.85 (SD 14.66)	1.02 (95 %-CI:0.98,1.05)	0.341
time between symptom onlapse and first CT scan (days)	7 (IQR 5–8.5)	7 (IQR 5–7)	0.89 (95 %-CI:0.71,1.1)	0.296
gender				
male	17 (42 %)	23 (58 %)		
female	14 (58 %)	10 (42 %)	0.53 (95 %-CI:0.19,1.46)	0.222
symptoms				
fever*				
no	6 (38 %)	10 (62 %)		
yes	25 (53 %)	22 (47 %)	0.53 (95 %-CI:0.16,1.66)	0.282
cough*				
no	6 (46 %)	7 (54 %)		
yes	23 (48 %)	25 (52 %)	0.93 (95 %-CI:0.26,3.21)	0.91
dyspnea*				
no	13 (68 %)	6 (32 %)		
yes	16 (39 %)	25 (61 %)	3.39 (95 %-CI:1.1,11.38)	**0.038**
fatigue*				
no	5 (38 %)	8 (62 %)		
yes	17 (50 %)	17 (50 %)	0.63 (95 %-CI:0.16,2.27)	0.48
gastrointestinal*				
no	16 (48 %)	17 (52 %)		
yes	5 (42 %)	7 (58 %)	1.32 (95 %-CI:0.35,5.27)	0.686
taste dysfunction*				
no	18 (55 %)	15 (45 %)		
yes	4 (36 %)	7 (64 %)	2.1 (95 %-CI:0.53,9.34)	0.301
comorbidities				
diabetes*				
no	27 (48 %)	29 (52 %)		
yes	4 (50 %)	4 (50 %)	0.93 (95 %-CI:0.2,4.29)	0.925
cardiac failure*				
no	29 (48 %)	32 (52 %)		
yes	2 (67 %)	1 (33 %)	0.45 (95 %-CI:0.02,4.97)	0.527
coronary heart disease*				
no	28 (48 %)	30 (52 %)		
yes	3 (50 %)	3 (50 %)	0.93 (95 %-CI:0.16,5.41)	0.936
COPD*				
no	31 (50 %)	31 (50 %)		
yes	0 (0%)	2 (100 %)	n.c.	0.493#
asthma*				
no	30 (49 %)	31 (51 %)		
yes	1 (33 %)	2 (67 %)	1.94 (95 %-CI:0.18,42.94)	0.598
high blood pressure*				
no	21 (52 %)	19 (48 %)		
yes	9 (39 %)	14 (61 %)	1.72 (95 %-CI:0.61,5)	0.308

COPD = chronic obstructive pulmonary disease.
* Occasional missing values were counted as patients without symptoms, #p-value of Fishers exact test due to quasi separated data.

n.c., p = 0.002) (Fig. 6), air bronchogram (Figs. 3, 5 and 6) (OR 4.22, 95 %-CI:1.41, 13.94, p = 0.013), pleural effusion (OR 4.06, 95 %-CI:1.09,19.71, p = 0.05) and vessel enlargement (OR 3.67, 95 %-CI:1.34, 10.71, p = 0.014) (Fig. 7). Also, bilateral lesions (OR n.c., p = 0.004), involvement of one of the upper lobes (right upper lobe: OR n.c., p = 0.004, left upper lobe OR 7.38, 95 %-CI:1.73, 51.29, p = 0.015) or of the right middle lobe (OR n.c., p < 0.001) were significantly more often seen in group 2. Moreover, extent of parenchymal opacifications of more than 66 % of lung volume predicted an unfavourable course of disease (OR 14.62, 95 %-CI:3.13, 108.96, p = 0.002) (Fig. 3). Results are presented in Table 4.

3.4. Multivariable analysis for identification of prognostic relevant CT features

Multivariable logistic regression including significant CT findings and distribution patterns from univariable analysis was performed to identify independent parameters for prediction of outcome. In order to avoid overfitting of the model and to keep the number of events per variable (EPV) large enough, the number of parameters included into the multivariable analysis was restricted as described in Material and Methods. Thus, two multivariable analyses were performed by grouping the parameters according to clinical considerations. Independent predictors for a negative outcome were crazy paving (OR 8.9, 95 %-CI: 1.64, 48.1, p = 0.011) and involvement of more than 66 % of lung parenchyma (OR 6.04, 95 %-CI: 1.12, 32.6, p = 0.034). Results are presented in Tables 5a and 5b.

4. Discussion

Prognosis of COVID-19 pneumonia is highly variable. While circa 80 % of patients show only mild or even no symptoms, 20 % suffer from severe or even critical disease and eventually die [4]. Identification of factors predicting prognosis already in the early phase of disease would enable physicians to direct patients into optimal therapeutic pathways. Health care resources could be employed precisely where they are needed most. CT plays a major role in the care of patients infected with SARS-CoV-2. Few studies investigated if CT might be helpful in

Fig. 4. Unilateral disease. Axial reconstruction of a CT in lung window demonstrating unilateral ground glass opacifications in the right lower lobe (arrow). Note also incidental scaring in the lingual segment.

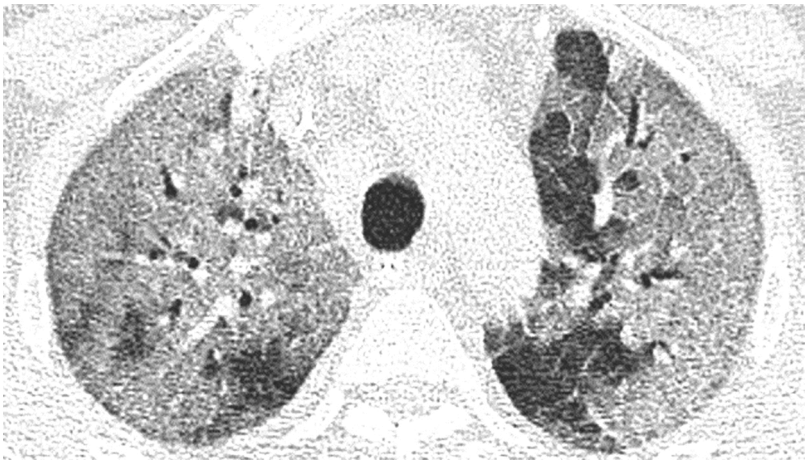

Fig. 5. Crazy paving. Axial reconstruction of a CT in lung window demonstrating extensive crazy paving in a patient with severe disease extent. Also note the air bronchogram.

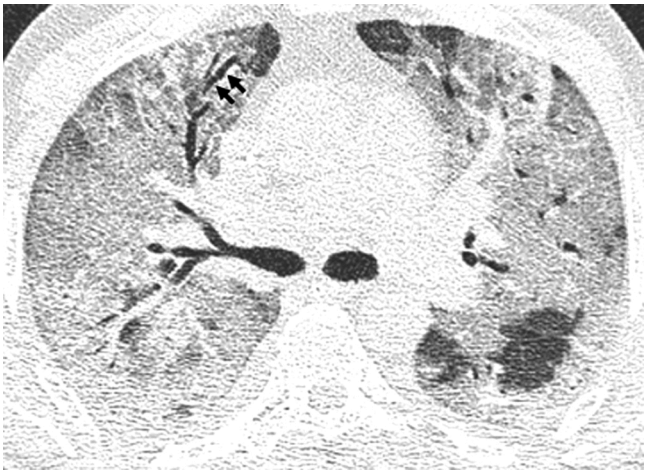

Fig. 6. Bronchial dilatation. Axial reconstruction of a CT in lung window showing a dilated bronchus within ground glass opacities (arrows). Also note the air bronchogram.

predicting prognosis [20–24]. However, most of the studies are from China. Evaluation of European cohorts in this regard is scarce [25]. Considering that outcome is influenced by many factors (eg health care resources, organization and preparedness of health care systems, host factors and viral factors influenced for example by genomic variations) we sought to investigate CT features predicting patient prognosis in a German cohort.

For this we evaluated a cohort of 64 patients with RT-PCR proven COVID-19 pneumonia treated at two tertiary care centers in Regensburg, Southern Germany. We restricted the analysis to CTs performed in the early disease phase (within 10 days of symptom onset). CT morphology of the presented cohort was in accordance with previously described features. A combination of bilateral GGO and consolidation located in the periphery of the posterior segments predominantly of the lower lobes was most often seen and seems to be characteristic for COVID-19 pneumonia. For identification of prognostic parameters patients were divided in two groups (group 1 with favorable outcome defined as care on regular ward or discharge, group 2 with unfavorable outcome defined as need for mechanical ventilation, admission to ICU, ECMO therapy or death). None of the analyzed demographic parameters and no comorbidity influenced patient outcome. In particular neither age nor male gender (which has been reported to be a risk factor by other groups) were of prognostic relevance in our cohort [22,28–30]. Regarding clinical symptoms, patients presenting with dyspnea at admission had a significantly worse outcome compared to patients without dyspnea. Also, univariable analysis identified several CT parameters which were associated with an adverse outcome, namely consolidation, crazy paving, geographic shape of opacities, dilatation of bronchi, air bronchogram, vessel enlargement and the presence of pleural effusions. Moreover, involvement of both lungs as well as the upper lobes and the right middle lobe were predictive for an unfavorable course of disease. Also, amount of opacifications more than 66 % of lung volume correlated highly significant with an adverse outcome. Conversely, unilateral disease predicted a benign course of disease. These findings are in accordance with the results of other studies. Several groups from China also reported crazy paving, bronchial dilatation, air bronchogram and extent of opacifications to be associated with an adverse outcome [22,21,24,23,31].

At first glance the presented results and data from literature suggest that outcome of patients suffering from COVID-19 pneumonia might be predicted by several different CT features. But, none of the other authors performed a multivariable analysis. We suspected that the significance of some features can be linked to the extent of parenchymal involvement: COVID-19 pneumonia initially manifests in form of predominant ground glass opacities and possibly minor consolidation in the periphery of the lower lobes. When opacifications increase in extent they gradually involve more segments. Thus, seemingly prognostic parameters like affection of the upper lobes and the right middle lobe might merely indicate increasing disease extent. Likewise it is not surprising that pleural effusion was significantly more prevalent in group 2. Also, there might be a link between crazy paving and geographic shape of opacifications both of which are well known CT features of acute respiratory distress syndrome (ARDS) which is seen in severe cases of COVID-19 pneumonia. To test for our hypothesis we performed a multivariable regression analysis. The results revealed that in our cohort crazy paving was the only CT feature that independently predicted an unfavorable course of disease. The differential diagnosis of crazy paving is wide and includes pulmonary edema and ARDS [32,33]. Both phenomena are thought to be the major pathophysiological events in severe COVID-19 pneumonia [34]. Thus, crazy paving might be an easy to assess surrogate parameter for severe lung injury by COVID-19 pneumonia. The presence of consolidation and bronchial dilatation did not reach statistical significance but showed a tendency for predicting a poor outcome. Bronchial dilatation or bronchiectasis can also be linked to ARDS being a consequence of fibroproliferative processes in the surrounding lung tissue during the proliferative, second phase [35,36]. Hence, bronchial dilatation might have been a surrogate for such a tissue response with an immanent adverse outcome. Another strong independent predictor for a

Fig. 7. Vessel enlargement. Axial reconstruction of a CT in lung window demonstrating a dilated vessel within a focal ground glass opacity (arrows).

Table 4
Univariable logistic regression to analyze the predictive value of CT features on the primary endpoint (positive vs. negative outcome).

CT findings	group 1 (n = 31)	group 2 (n = 33)	odds ratio	p-value
GGO				
no	2 (100 %)	0 (0%)		
yes	29 (47 %)	33 (53 %)	n.c.	0.231[#]
consolidation				
no	11 (73 %)	4 (27 %)		
yes	20 (41 %)	29 (59 %)	3.99 (95 %-CI:1.18,16.06)	**0.034**
crazy paving				
no	29 (60 %)	19 (40 %)		
yes	2 (12 %)	14 (88 %)	10.68 (95 %-CI:2.6,73.12)	**0.004**
round shape of opacification				
no	9 (36 %)	16 (64 %)		
yes	22 (56 %)	17 (44 %)	0.43 (95 %-CI:0.15,1.2)	0.114
sharp margin of opacification				
no	6 (60 %)	4 (40 %)		
yes	25 (46 %)	29 (54 %)	1.74 (95 %-CI:0.45,7.47)	0.429
geographic shape of opacification				
no	23 (61 %)	15 (39 %)		
yes	8 (31 %)	18 (69 %)	3.45 (95 %-CI:1.23,10.35)	**0.022**
curvilinear/bandlike opacification				
no	22 (49 %)	23 (51 %)		
yes	9 (47 %)	10 (53 %)	1.06 (95 %-CI:0.36,3.16)	0.911
bronchial dilatation				
no	31 (56 %)	24 (44 %)		
yes	0 (0%)	9 (100 %)	n.c.	**0.002**[#]
air bronchogram				
no	15 (71 %)	6 (29 %)		
yes	16 (37 %)	27 (63 %)	4.22 (95 %-CI:1.41,13.94)	**0.013**
cavitation				
no	31 (48 %)	33 (52 %)	n.c.	n.c.
vessel enlargment				
no	21 (64 %)	12 (36 %)		
yes	10 (32 %)	21 (68 %)	3.67 (95 %-CI:1.34,10.71)	**0.014**
pleural effusion				
no	28 (55 %)	23 (45 %)		
yes	3 (23 %)	10 (77 %)	4.06 (95 %-CI:1.09,19.71)	**0.050**
lymphadenopathy				
no	24 (52 %)	22 (48 %)		
yes	7 (39 %)	11 (61 %)	1.71 (95 %-CI:0.57,5.41)	0.341
unilateral				
no	26 (44 %)	33 (56 %)		
yes	5 (100 %)	0 (0%)	n.c.	**0.022**[#]
bilateral				
no	7 (100 %)	0 (0%)		
yes	24 (42 %)	33 (58 %)	n.c.	**0.004**[#]
right upper lobe				
no	7 (100 %)	0 (0%)		
yes	24 (42 %)	33 (58 %)	n.c.	**0.004**[#]
right middle lobe				
no	10 (100 %)	0 (0%)		
yes	21 (39 %)	33 (61 %)	n.c.	**<0.001**[#]
right lower lobe				
no	3 (100 %)	0 (0%)		
yes	28 (46 %)	33 (54 %)	n.c.	0.108[#]
left upper lobe				
no	10 (83 %)	2 (17 %)		
yes	21 (40 %)	31 (60 %)	7.38 (95 %-CI:1.73,51.29)	**0.015**
left lower lobe				
no	4 (80 %)	1 (20 %)		
yes	27 (46 %)	32 (54 %)	4.74 (95 %-CI:0.65,95.75)	0.175
peripheral				
no	6 (35 %)	11 (65 %)		
yes	25 (53 %)	22 (47 %)	0.48 (95 %-CI:0.14,1.48)	0.210
central				
no	31 (48 %)	33 (52 %)	n.c.	n.c.
diffuse				
no	21 (54 %)	18 (46 %)		
yes	10 (40 %)	15 (60 %)	1.75 (95 %-CI:0.64,4.95)	0.281
predominantly anterior				
no	30 (48 %)	32 (52 %)		
yes	1 (50 %)	1 (50 %)	0.94 (95 %-CI:0.04,24.42)	0.964
predominantly posterior				
no	5 (45 %)	6 (55 %)		
yes	26 (49 %)	27 (51 %)	0.87 (95 %-CI:0.22,3.21)	0.828
extent of lung involvement				
mild	18 (69 %)	8 (31 %)	reference	
moderate	11 (48 %)	12 (52 %)	2.45 (95 %-CI:0.78,8.17)	0.132
severe	2 (13 %)	13 (87 %)	14.62 (95 %-CI:3.13,108.96)	**0.002**
contrast agent				
enhanced scans	7 (54 %)	6 (46 %)		
unenhanced scans	24 (47 %)	27 (53 %)		

n.c.: not computable due to quasi separated data.
[#] p-value of Fishers exact test due to quasi separated data.

Table 5a
Multivariable logistic regression to analyze the predictive value of significant CT features on the primary endpoint (positive vs. negative outcome).

parameter	odds ratio[*]	p-value[*]
crazy paving	8.9 (95 %-CI: 1.64, 48.1)	0.011
bronchial dilatation	23.5 (95 %-CI: 0.81, 684)	0.066
consolidation	4.52 (95 %-CI: 0.98, 20.9)	0.054

[*] Odds ratios and p-values were estimated by the penalized likelihood method by Firth.

Table 5b
Multivariable logistic regression to analyze the predictive value of significant characteristics of parenchymal involvement on the endpoint (positive vs. negative outcome).

parameter	odds ratio*	p-value*
involvement right middle lobe	19.1 (95 %-CI: 0.89, 410)	0.060
extent of disease		
mild	reference	
moderate	1.33 (95 %-CI: 0.38, 4.68)	0.311
severe	6.04 (95 %-CI: 1.12, 32.6)	0.034

* Odds ratios and p-values were estimated by the penalized likelihood method by Firth.

poor outcome was severity of parenchymal involvement even though extent of parenchymal involvement was assessed subjectively.

Our study has limitations. CT scans were performed at the discretion of the referring physician. Hence, there might be a bias towards seriously ill patients. Both recruiting hospitals were tertiary care institutions with one of them being the regional center for critically ill patients. Thus, the proportion of patients with moderately to severely involved lung parenchyma was relatively high. Differences in treatment were not systematically analyzed.

5. Conclusion

We investigated the prognostic relevance of chest CT performed in the early phase of disease for 64 patients from Germany suffering from RT-PCR proven COVID-19 pneumonia. Independent predictors for an adverse outcome were crazy paving and severe parenchymal involvement. These are easy to asses CT parameters. Hence, CT might be a valuable modality to predict the course of disease and to help clinicians to adapt patient management accordingly.

CRediT authorship contribution statement

Stefanie Meiler: Investigation, Data curation, Writing - original draft, Visualization. **Jan Schaible:** Investigation, Data curation. **Florian Poschenrieder:** Conceptualization, Methodology, Project administration. **Gregor Scharf:** Software. **Florian Zeman:** Software, Formal analysis, Visualization. **Janine Rennert:** Methodology, Investigation. **Benedikt Pregler:** Investigation. **Henning Kleine:** Investigation. **Christian Stroszczynski:** Resources, Supervision. **Niels Zorger:** Resources, Supervision. **Okka W. Hamer:** Conceptualization, Methodology, Validation, Writing - review & editing, Supervision, Project administration.

Declaration of Competing Interest

The authors report no declarations of interest.

References

[1] N. Zhu, D. Zhang, W. Wang, X. Li, B. Yang, J. Song, et al., A novel coronavirus from patients with pneumonia in China, 2019, N. Engl. J. Med. 382 (2020) 727–733, https://doi.org/10.1056/NEJMoa2001017.

[2] World Health Organization, WHO Announces COVID-19 Outbreak a Pandemic, 2020 (Accessed 2 May 2020), http://www.euro.who.int/en/health-topics/health-emergencies/coronavirus-covid-19/news/news/2020/3/who-announces-covid-19-outbreak-a-pandemic.

[3] Johns Hopkins University & Medicine, COVID-19 Dashboard by the Center for Systems Science and Engineering (CSSE) at Johns Hopkins University (JHU), 2020 (Accessed 29 June 2020), https://coronavirus.jhu.edu/map.html.

[4] Z. Wu, J.M. McGoogan, Characteristics of and important lessons from the Coronavirus Disease 2019 (COVID-19) outbreak in China: summary of a report of 72314 cases from the Chinese center for disease control and prevention, JAMA 323 (2020) 1239–1242, https://doi.org/10.1001/jama.2020.2648.

[5] D. Caruso, M. Zerunian, M. Polici, F. Pucciarelli, T. Polidori, C. Rucci, et al., Chest CT Features of COVID-19 in Rome, Italy, Radiology (2020), 201237, https://doi.org/10.1148/radiol.2020201237.

[6] M. Chung, A. Bernheim, X. Mei, N. Zhang, M. Huang, X. Zeng, et al., CT imaging features of 2019 novel coronavirus (2019-nCoV), Radiology 295 (2020) 202–207, https://doi.org/10.1148/radiol.2020200230.

[7] Y.-N. Duan, J. Qin, Pre- and posttreatment chest CT findings: 2019 novel coronavirus (2019-nCoV) pneumonia, Radiology 295 (2020) 21, https://doi.org/10.1148/radiol.2020200323.

[8] R. Han, L. Huang, H. Jiang, J. Dong, H. Peng, D. Zhang, Early clinical and CT manifestations of coronavirus disease 2019 (COVID-19) pneumonia, AJR Am. J. Roentgenol. (2020) 1–6, https://doi.org/10.2214/AJR.20.22961.

[9] W. Kong, P.P. Agarwal, Chest imaging appearance of COVID-19 infection, Radiol.: Cardiothorac. Imaging 2 (2020) e200028, https://doi.org/10.1148/ryct.2020200028.

[10] Z. Ye, Y. Zhang, Y. Wang, Z. Huang, B. Song, Chest CT manifestations of new coronavirus disease 2019 (COVID-19): a pictorial review, Eur. Radiol. 30 (2020) 4381–4389, https://doi.org/10.1007/s00330-020-06801-0.

[11] O.W. Hamer, B. Salzberger, J. Gebauer, C. Stroszczynski, M. Pfeifer, CT-Morphologie von COVID-19: Fallbeispiel und Literaturübersicht, Fortschr. Röntgenstr. 192 (2020) 386–392, https://doi.org/10.1055/a-1142-4094.

[12] H. Wang, R. Wei, G. Rao, J. Zhu, B. Song, Characteristic CT findings distinguishing 2019 novel coronavirus disease (COVID-19) from influenza pneumonia, Eur. Radiol. 30 (2020) 4910–4917, https://doi.org/10.1007/s00330-020-06880-z.

[13] M. Liu, W. Zeng, Y. Wen, Y. Zheng, F. Lv, K. Xiao, COVID-19 pneumonia: CT findings of 122 patients and differentiation from influenza pneumonia, Eur. Radiol. 30 (2020) 1–7, https://doi.org/10.1007/s00330-020-06928-0.

[14] L. Luo, Z. Luo, Y. Jia, C. Zhou, J. He, J. Lyu, X. Shen, CT differential diagnosis of COVID-19 and non-COVID-19 in symptomatic suspects: a practical scoring method, BMC Pulm. Med. 20 (2020) 129, https://doi.org/10.1186/s12890-020-1170-6.

[15] H.X. Bai, B. Hsieh, Z. Xiong, K. Halsey, J.W. Choi, T.M.L. Tran, et al., Performance of radiologists in differentiating COVID-19 from viral pneumonia on chest CT, Radiology (2020), 200823, https://doi.org/10.1148/radiol.2020200823.

[17] T. Ai, Z. Yang, H. Hou, C. Zhan, C. Chen, W. Lv, et al., Correlation of chest CT and RT-PCR testing in coronavirus disease 2019 (COVID-19) in China: a report of 1014 cases, Radiology (2020), 200642, https://doi.org/10.1148/radiol.2020200642.

[18] Y. Fang, H. Zhang, J. Xie, M. Lin, L. Ying, P. Pang, W. Ji, Sensitivity of chest CT for COVID-19: comparison to RT-PCR, Radiology (2020), 200432, https://doi.org/10.1148/radiol.2020200432.

[19] X. Xie, Z. Zhong, W. Zhao, C. Zheng, F. Wang, J. Liu, Chest CT for typical 2019-nCoV pneumonia: relationship to negative RT-PCR testing, Radiology (2020), 200343, https://doi.org/10.1148/radiol.2020200343.

[20] S.M.H. Tabatabaei, H. Talari, F. Moghaddas, H. Rajebi, Computed tomographic features and short-term prognosis of coronavirus disease 2019 (COVID-19) pneumonia: a single-center study from Kashan, Iran, Radiol.: Cardiothorac. Imaging 2 (2020) e200130, https://doi.org/10.1148/ryct.2020200130.

[21] K. Li, J. Wu, F. Wu, D. Guo, L. Chen, Z. Fang, C. Li, The clinical and chest CT features associated with severe and critical COVID-19 pneumonia, Invest. Radiol. 55 (2020) 327–331, https://doi.org/10.1097/RLI.0000000000000672.

[22] W. Zhao, Z. Zhong, X. Xie, Q. Yu, J. Liu, Relation between chest CT findings and clinical conditions of coronavirus disease (COVID-19) pneumonia: a multicenter study, AJR Am. J. Roentgenol. (2020) 1–6, https://doi.org/10.2214/AJR.20.22976.

[23] M. Yuan, W. Yin, Z. Tao, W. Tan, Y. Hu, Association of radiologic findings with mortality of patients infected with 2019 novel coronavirus in Wuhan, China, PLoS One 15 (2020) e0230548, https://doi.org/10.1371/journal.pone.0230548.

[24] P. Lyu, X. Liu, R. Zhang, L. Shi, J. Gao, The performance of chest CT in evaluating the clinical severity of COVID-19 pneumonia: identifying critical cases based on CT characteristics, Invest. Radiol. 55 (2020) 412–421, https://doi.org/10.1097/RLI.0000000000000689.

[25] D. Colombi, F.C. Bodini, M. Petrini, G. Maffi, N. Morelli, G. Milanese, et al., Well-aerated lung on admitting chest CT to predict adverse outcome in COVID-19 pneumonia, Radiology (2020), 201433, https://doi.org/10.1148/radiol.2020201433.

[26] D.M. Hansell, A.A. Bankier, H. MacMahon, T.C. McLoud, N.L. Müller, J. Remy, Fleischner society: glossary of terms for thoracic imaging, Radiology 246 (2008) 697–722, https://doi.org/10.1148/radiol.2462070712.

[27] D. FIRTH, Bias reduction of maximum likelihood estimates, Biometrika 80 (1993) 27, https://doi.org/10.2307/2336755.

[28] M. Yu, D. Xu, L. Lan, M. Tu, R. Liao, S. Cai, et al., Thin-section chest CT imaging of coronavirus disease 2019 pneumonia: comparison between patients with mild and severe disease, Radiol.: Cardiothorac. Imaging 2 (2020) e200126, https://doi.org/10.1148/ryct.2020200126.

[29] C. Huang, Y. Wang, X. Li, L. Ren, J. Zhao, Y. Hu, et al., Clinical features of patients infected with 2019 novel coronavirus in Wuhan, China, Lancet 395 (2020) 497–506, https://doi.org/10.1016/S0140-6736(20)30183-5.

[30] Y. Meng, P. Wu, W. Lu, K. Liu, K. Ma, L. Huang, et al., Sex-specific clinical characteristics and prognosis of coronavirus disease-19 infection in Wuhan, China: a retrospective study of 168 severe patients, PLoS Pathog. 16 (2020), e1008520, https://doi.org/10.1371/journal.ppat.1008520.

[31] S.M.H. Tabatabaei, H. Talari, F. Moghaddas, H. Rajebi, Computed tomographic features and short-term prognosis of coronavirus disease 2019 (COVID-19) pneumonia: a single-center study from Kashan, Iran, Radiol.: Cardiothorac. Imaging 2 (2020) e200130, https://doi.org/10.1148/ryct.2020200130.

[32] W. de Wever, J. Meersschaert, J. Coolen, E. Verbeken, J.A. Verschakelen, The crazy-paving pattern: a radiological-pathological correlation, Insights Imaging 2 (2011) 117–132, https://doi.org/10.1007/s13244-010-0060-5.

[33] S.E. Rossi, J.J. Erasmus, M. Volpacchio, T. Franquet, T. Castiglioni, H.P. McAdams, "Crazy-paving" pattern at thin-section CT of the lungs: radiologic-pathologic

overview, Radiographics 23 (2003) 1509–1519, https://doi.org/10.1148/rg.236035101.
[34] M.Z. Tay, C.M. Poh, L. Rénia, P.A. MacAry, L.F.P. Ng, The trinity of COVID-19: immunity, inflammation and intervention, Nat. Rev. Immunol. 20 (2020) 363–374, https://doi.org/10.1038/s41577-020-0311-8.
[35] E.L. Burnham, W.J. Janssen, D.W.H. Riches, M. Moss, G.P. Downey, The fibroproliferative response in acute respiratory distress syndrome: mechanisms and clinical significance, Eur. Respir. J. 43 (2014) 276–285, https://doi.org/10.1183/09031936.00196412.
[36] B.T. Thompson, R.C. Chambers, K.D. Liu, Acute respiratory distress syndrome, N. Engl. J. Med. 377 (2017) 562–572, https://doi.org/10.1056/NEJMra1608077.